

## Research Article

# Alignment of TiO<sub>2</sub> (Anatase) Crystal of Dye-Sensitized Solar Cells by External Magnetic Field

**Na-Yeong Hong, Hyunwoong Seo, Min-Kyu Son, Soo-Kyoung Kim, Song-Yi Park, Kandasamy Prabakar, and Hee-Je Kim**

*Department of Electrical Engineering, Pusan National University, Pusan 609-735, Republic of Korea*

Correspondence should be addressed to Hee-Je Kim; [heeje@pusan.ac.kr](mailto:heeje@pusan.ac.kr)

Received 6 February 2013; Revised 23 May 2013; Accepted 25 May 2013

Academic Editor: Tianxin Wei

Copyright © 2013 Na-Yeong Hong et al. This is an open access article distributed under the Creative Commons Attribution License, which permits unrestricted use, distribution, and reproduction in any medium, provided the original work is properly cited.

In this study, magnetic field ( $B$ ) was applied on TiO<sub>2</sub> (anatase) of dye-sensitized solar cell (DSC) for alignment of crystal. Magnetic field was applied on TiO<sub>2</sub> when deposited TiO<sub>2</sub> on the fluorine tin oxide (FTO) was dried at 373 K for crystalline orientation. And applying time of  $B$  was varied 0~25 min. Characteristics of the magnetic field applied TiO<sub>2</sub> films were analyzed by X-ray diffraction (XRD), high resolution transmission electron microscopy (HRTEM), scanning electron microscopy (SEM), and electrochemical impedance spectroscopy (EIS). Current-voltage characteristics were also analyzed using solar simulator, and it was confirmed that the energy conversion efficiency of 41% was increased. Finally, it was identified that the magnetic field affected orientation of TiO<sub>2</sub>, resulting in the enhancement of the performance of the DSC.

## 1. Introduction

DSC is one of the promising alternatives to conventional solar cells because of low fabrication cost and relatively simple production processes. A typical DSC is a sandwich structure which consists of a nanoporous TiO<sub>2</sub> film photoelectrode covered with a monolayer of the Ruthenium complex-based dye, a Pt counterelectrode, and a redox electrolyte of I<sup>-</sup>/I<sub>3</sub><sup>-</sup> in an acetonitrile solution which is between two electrodes [1, 2].

Semiconductor of photoelectrode is important role in DSC performance, because electrons from dye molecules transport to conductive glass through semiconductor materials by hopping. To enhance dye absorption and accessibility to the hole-carrying electrolyte, a mesoporous structure is essential for the semiconductor film [3]. However, mesoporous films are of a nanocrystalline nature and contain numerous crystal defects in the grain boundaries. These defects impede electron transport and are harmful to cell performance [4–8]. The diffusion of electrons through the nanocrystalline network is several orders of magnitude slower than that in a single crystal [9]. Thus, how the crystal structure of nanocrystalline films affects electron transport is an important issue.

Among the semiconductor materials used in DSCs [10–12], TiO<sub>2</sub> has been proven to be the best semiconductor material for the DSC. TiO<sub>2</sub> has three crystallographic polymorphs, that is, rutile, anatase, and brookite, composed of Ti ions having octahedral coordination. Anatase is perceived as the more active phase of TiO<sub>2</sub> because of its surface chemistry and potentially higher conduction-band edge energy [13] and shows advantages in photocatalysis and energy conversion. The size, shape, crystallization, and morphology of anatase particles are important to the performance of the DSC, because this has a great effect on electron mobility and then energy conversion efficiency. Generally, TiO<sub>2</sub> in DSC has nanoporous structure. It is advantageous for dye absorbing but causes many losses of energy.

It has been reported that anatase has an orientation dependence of the reaction activity. Water reduction and photooxidation occur at more negative potentials for the anatase (0 0 1) surface than for the anatase (1 0 1) surface [14]. Orienting anatase nanocrystals with (0 0 1) preferred growth may improve the electron transport in the nanoporous structured dye-sensitized solar cells by changing structure of the photoelectrode [15].

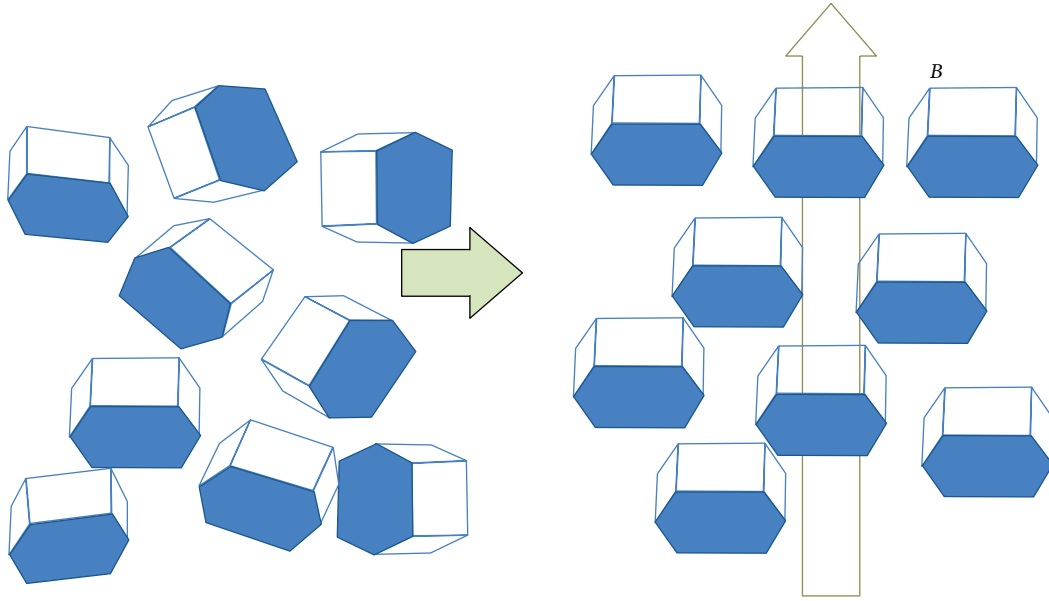


FIGURE 1: Concept of the well-aligned  $\text{TiO}_2$  crystals in magnetic field.

Many materials including  $\text{TiO}_2$  in asymmetric crystalline structures have anisotropic magnetic susceptibilities, associated with their crystal structures as in

$$\Delta\chi = \chi_{\parallel} - \chi_{\perp}, \quad (1)$$

where  $\chi_{\parallel}$  and  $\chi_{\perp}$  are the susceptibilities parallel and perpendicular to the magnetic principal axis, respectively.

The driving force of the magnetic alignment is the energy of the crystal anisotropy and is given as

$$\Delta E = \frac{\Delta\chi VB^2}{2\mu_0}, \quad (2)$$

where  $V$  is the volume of the material,  $B$  is the applied magnetic field, and  $\mu_0$  is the permeability in a vacuum [16]. Therefore, when a single crystal of anatase  $\text{TiO}_2$  is placed in a magnetic field, the crystal is rotated, and the crystallographic axis of high  $\chi$  is aligned in the direction of the magnetic field. A schematic illustration of the rotation of particles in a magnetic field is shown in Figure 1 [17]. It is expected that this property provides  $\text{TiO}_2$  photoelectrode condition advantageous for electron transport.

In this study, we researched the alignment of  $\text{TiO}_2$  (anatase) crystal in the DSC by applying the external magnetic field. Characteristics of the magnetic field applied  $\text{TiO}_2$  films were analyzed by X-ray diffraction (XRD), high resolution transmission electron microscopy (HRTEM), scanning electron microscopy (SEM), UV-vis spectroscopy, and electrochemical impedance spectroscopy (EIS). And current-voltage characteristics were analyzed using solar simulator. As a result, it was confirmed that the energy conversion efficiency was enhanced by the well-aligned anatase  $\text{TiO}_2$  crystal, resulting from the external magnetic field.

## 2. Experimental

**2.1. Preparation of the Photoelectrode.**  $\text{TiO}_2$  paste (Ti-Nanoxide HT/SP, Solaronix) was deposited on FTO glass by the doctor-blade method (effective area =  $0.29 \text{ cm}^2$ ). And then, magnetic field was applied by setting the photoelectrode between two permanent Neodymium magnets when the paste was dried at 373 K. The magnetic flux density was 2.99 T measured by Gauss Meter (MG4D, WALKER). Applying time of magnetic field was varied 0, 5, 10, and 25 min. After that, the photoelectrodes were calcined at 723 K for 30 min to form porosity. It was immersed in 0.5 mM N719 dye ( $\text{Ru}(2,20\text{-bipyridyl-4,40-dicarboxylate})_2(\text{NCS})_2$ , Solaronix) solution for 24 h, so that dye molecules are attached to  $\text{TiO}_2$ . Then photoelectrode was rinsed with ethyl alcohol for the excess dye molecule elimination and dried.

**2.2. DSC Fabrication.** Pt counterelectrode was prepared with depositing Pt paste (Pt-Catalyst T/SP, Solaronix) by the doctor-blade method on the FTO glass which has predrilled pin holes to inject electrolyte and sintered at 723 K for 10 min. Prepared two electrodes were joined with thermoplastic hot-melt sheet (SX 1170-60, Solaronix). Electrolyte (0.5 M LiI, 0.05 M  $\text{I}_2$ , and 0.5 M 4-tert-butylpyridine) was injected between two electrodes, and holes were sealed with cover glass.

**2.3. Characterizations.** The morphology and the structure of the  $\text{TiO}_2$  film were investigated by high resolution transmission electron microscopy (HRTEM, Jem 2011, Jeol Cop.), field emission scanning electron microscopy (FE-SEM, S-4200, Hitachi), and X-ray diffraction (XRD, PANalytical B.V.). The performances of cell were tested by recording the current-voltage curve with source meter (Model 2400, Keithley Instrument, Inc.) under standard illumination

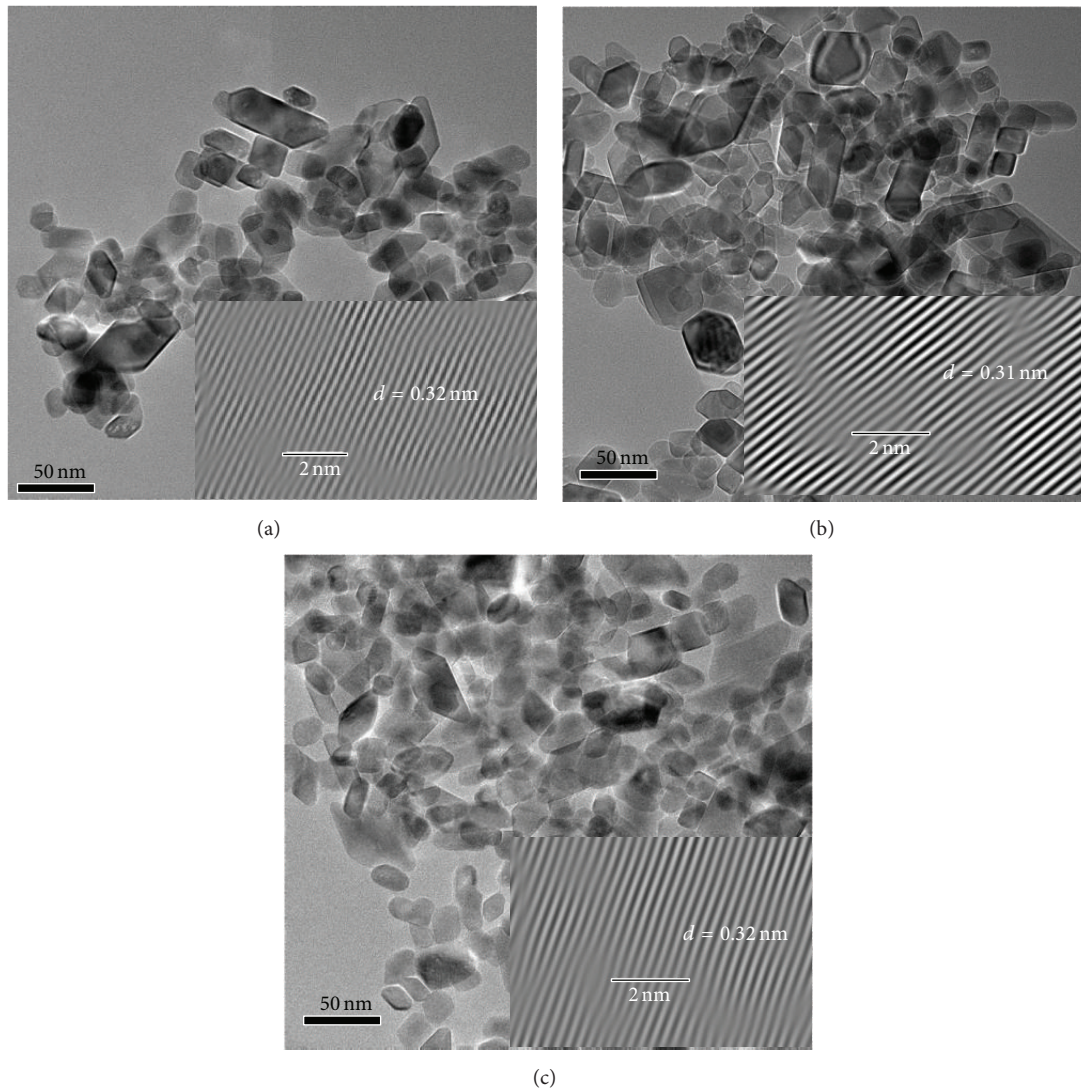


FIGURE 2: The HRTEM images of (a) the conventional  $\text{TiO}_2$ , (b) the magnetic field applied  $\text{TiO}_2$  after calcined at 723 K for 30 min, and (c) the magnetic field applied  $\text{TiO}_2$  without sintering.

of 1 sun ( $100 \text{ mW/cm}^2$ , AM 1.5). The absorption spectra were obtained using a UV-vis spectrophotometer (Optizen 3220UV, Mecasys). Internal impedance of DSC was measured using electrochemical impedance spectroscopy (EIS, SP-150, Biologic SAS), with a frequency ranging  $10^{-2} \text{ Hz} \sim 10^6 \text{ Hz}$ .

### 3. Results and Discussion

**3.1. Morphology and Structure of  $\text{TiO}_2$ .** The HRTEM images of the conventional  $\text{TiO}_2$  (a), the magnetic field applied  $\text{TiO}_2$  after calcined at 723 K for 30 min (b), and the magnetic field applied  $\text{TiO}_2$  without sintering (c) were shown in Figure 2. The corresponding lattice fringes shown in the insets of all figures were clearly observed, indicating that  $\text{TiO}_2$  nanoparticles formed with good crystallinity. The interplanar spacing was determined to be 0.32, 0.31, and 0.32 nm, respectively. There was no big difference; it means magnetic field could not affect the structure of crystal.

Figure 3 is XRD patterns of the conventional  $\text{TiO}_2$ , the magnetic field applied  $\text{TiO}_2$  after calcined at 723 K for 30 min, and the magnetic field applied  $\text{TiO}_2$  without sintering. All shows anatase peaks. The diffraction peak of the (0 0 4) of both  $B$  applied anatase is stronger than that of conventional. This said that magnetic field made the (0 0 4) plane of anatase vertical to its direction. Anatase  $\text{TiO}_2$  particle has a tetragonal crystalline structure and is very likely to be aligned with the direction of the magnetic field as explained with formulae (1) and (2). The  $c$ -axis of the anatase  $\text{TiO}_2$  particle is aligned parallel to  $B$  in the suspension. This property is important for improving interparticle electrical contact and for transporting electrons at neck of interparticle connections [10]. Disordered crystals create defect states during nanoparticle necking into films. These defect states serve as electron trap states, retarding both the electron transport toward the FTO substrate and electron recombination with the electrolyte [4, 18]. And no difference between sintered

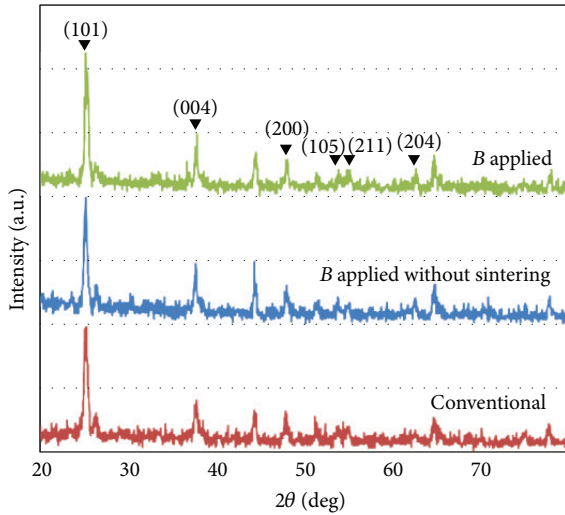


FIGURE 3: XRD patterns of conventional  $\text{TiO}_2$ ,  $B$  applied  $\text{TiO}_2$ , and  $B$  applied  $\text{TiO}_2$  without sintering.

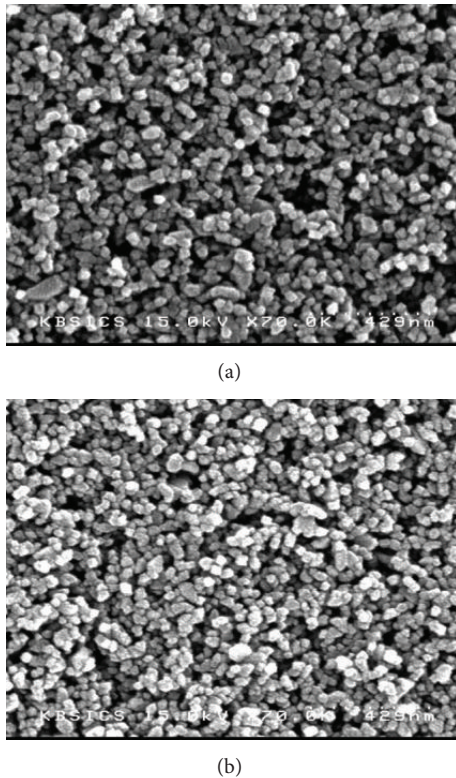


FIGURE 4: SEM images of reference  $\text{TiO}_2$  (a) and magnetic field applied  $\text{TiO}_2$  (b).

and not sintered  $B$  applied  $\text{TiO}_2$  was considered no alignment transform of crystals by calcination.

Figure 4 shows SEM images of conventional  $\text{TiO}_2$  and magnetic field applied  $\text{TiO}_2$  nanoparticles deposited on the FTO glass after calcined at 723 K for 30 min, (a) and (b), respectively. The diameter of each particle is in range of 20~30 nm in both images. It means that magnetic field did not

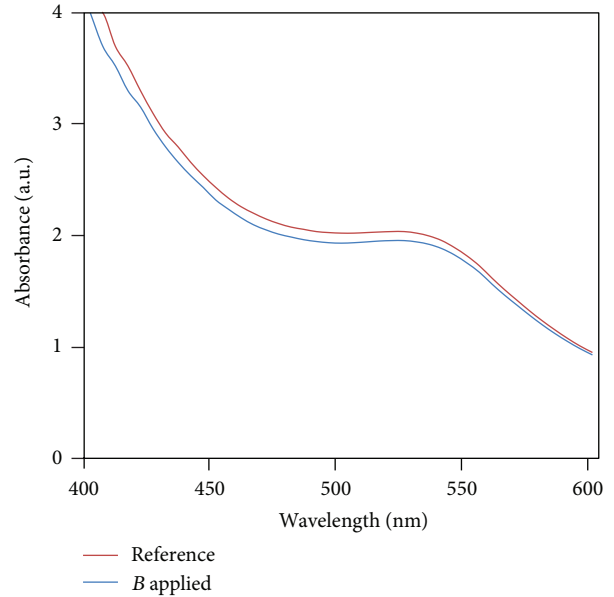


FIGURE 5: UV-vis absorption spectra of DSCs.

affect the size of particle. The morphology of conventional  $\text{TiO}_2$  is roughly packed and uneven. Compare to conventional one, the  $\text{TiO}_2$  film after crystallization assisted by magnetic field became more densely packed and flat. This shows that magnetic field aligned  $\text{TiO}_2$  crystals well.

Figure 5 is UV-vis absorption spectra of magnetic field applied and not applied DSCs. Because both used N719 dye, similar shapes of absorption spectra are shown. Magnetic field applied cell was densely packed comparable to conventional, therefore a surface area of  $\text{TiO}_2$  was decreased, and there were less voids to attach dye molecules. So the light absorption of  $B$  applied cell was decreased. Despite this, the photocurrent was increased by the well-oriented  $\text{TiO}_2$  that is discussed later.

**3.2. The Current-Voltage Behaviors.** Under standard illumination of 1 sun,  $I$ - $V$  curves of DSCs based on conventional and magnetic field applied  $\text{TiO}_2$  were measured. They are shown in Figure 6, and the photovoltaic characteristics of these DSCs are summarized in Table 1. Photocurrent was increased as applying time of magnetic field rises, while the open circuit voltage did not change noticeably. Higher photocurrent is probably related to the amount of absorbed dye, light scattering, or interparticle electrical contact. Although the dye absorption was decreased as magnetic field applying, photocurrent was increased. Well-aligned nanoparticles improved electrical contact so that electron transport became faster (Figure 7). When the magnetic field applying time was increased, photocurrent of DSC was enhanced. It says that crystal orientation is better with longer magnetic field applied time on  $\text{TiO}_2$ . As a result, the 7.50% efficiency of DSC with well-aligned  $\text{TiO}_2$  crystal by applying magnetic field for 25 min was 41% higher than the 5.31% efficiency for conventional. After 25 min, the  $\text{TiO}_2$  paste was fully dried,

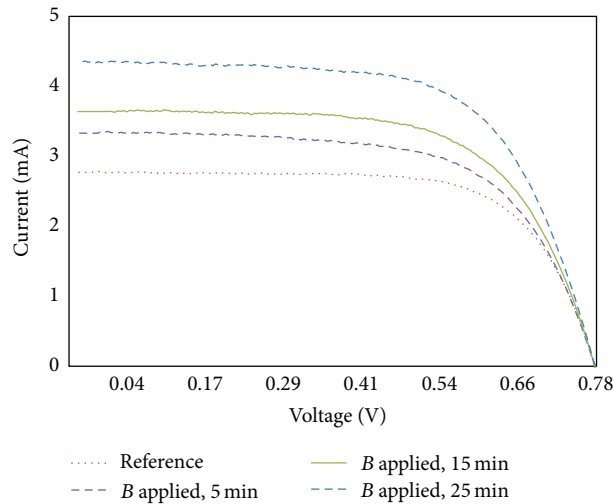


FIGURE 6: *I-V* curves of magnetic field applied DSCs with different applying times under standard illumination of 1 sun.

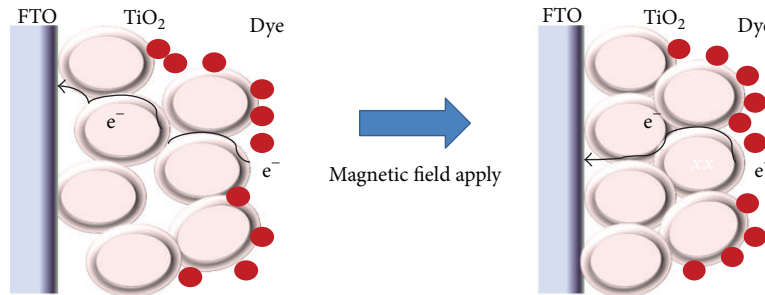


FIGURE 7: Schematic illustration of faster electron transportation in  $\text{TiO}_2$  nanocrystals after magnetic field applied.

TABLE 1: *I-V* characteristics of magnetic field applied DSCs of different applying times.

Applied time (min)	$V_{OC}$ (V)	$I_{SC}$ (mA)	FF	Efficiency (%)
0	0.80	2.79	0.69	5.31
5	0.79	3.43	0.62	5.79
15	0.79	3.75	0.62	6.33
25	0.78	4.36	0.64	7.50

and additional magnetic field did not change orientation of  $\text{TiO}_2$  particle. Therefore, additional  $B$  did not bring efficiency enhancement.

Electrochemical impedance spectra of magnetic field applied and not applied DSCs are shown in Figure 8.  $R_1$  (real part of small semicircle) is the electron transfer resistances at Pt/electrolyte interface, and  $R_2$  (real part of large semicircle) is at  $\text{TiO}_2$ /dye/electrolyte interface [19]. While  $R_1$  of two plots is similar, there is difference in  $R_2$ . Resistance of  $\text{TiO}_2$ /dye/electrolyte interface ( $R_2$ ) was decreased from  $44 \Omega$  to  $39 \Omega$  by applying magnetic field onto  $\text{TiO}_2$ . It implies that well-oriented  $\text{TiO}_2$  nanoparticles by applying magnetic field improved electron conductivity. Consequently, overall performance of DSC was enhanced.

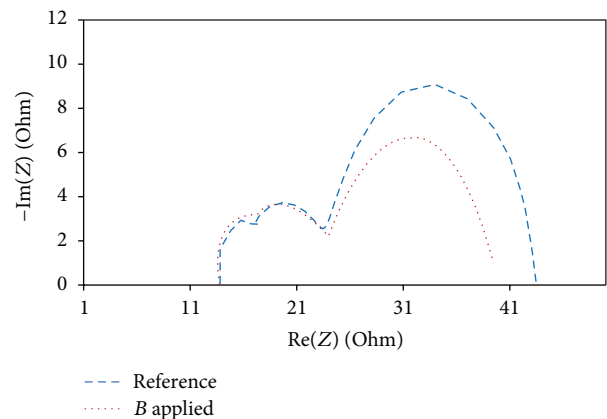


FIGURE 8: Internal resistances of the DSCs measured by EIS.

#### 4. Conclusions

In this study, effect of the magnetic field on anatase  $\text{TiO}_2$  crystal alignment of DSC was investigated. It was reported that the magnetic field arranges  $\text{TiO}_2$  crystal to its direction

that has advantage for reaction activity. The *c*-axis of the anatase TiO<sub>2</sub> is aligned parallel to *B* in the suspension. This improved interparticle electrical contact and for transporting electrons at neck of interparticle connections. It was identified with EIS that resistance of TiO<sub>2</sub>/dye/electrolyte interface (*R*<sub>2</sub>) was decreased by applying magnetic field onto TiO<sub>2</sub>. Consequently, it was demonstrated that energy conversion efficiency of TiO<sub>2</sub> particles arrangement was enhanced by an external magnetic field.

## Conflict of Interests

The authors declare no conflict of interests.

## Acknowledgment

This work no. 20110001295 was supported by Mid-Career Researcher Program through NRF grant funded by the MEST.

## References

- [1] B. O'Regan and M. Gratzel, "A low-cost, high-efficiency solar cell based on dye-sensitized colloidal TiO<sub>2</sub> films," *Nature*, vol. 353, pp. 737–740, 1991.
- [2] A. Hagfeldt and M. Gratzel, "Light-induced redox reactions in nanocrystalline systems," *Chemical Reviews*, vol. 95, no. 1, pp. 49–68, 1995.
- [3] C. J. Barbé, F. Arendse, P. Comte et al., "Nanocrystalline titanium oxide electrodes for photovoltaic applications," *Journal of the American Ceramic Society*, vol. 80, no. 12, pp. 3157–3171, 1997.
- [4] M. J. Cass, A. B. Walker, D. Martinez, and L. M. Peter, "Grain morphology and trapping effects on electron transport in dye-sensitized nanocrystalline solar cells," *Journal of Physical Chemistry B*, vol. 109, no. 11, pp. 5100–5107, 2005.
- [5] T. Oekermann, D. Zhang, T. Yoshida, and H. Minoura, "Electron transport and back reaction in nanocrystalline TiO<sub>2</sub> films prepared by hydrothermal crystallization," *Journal of Physical Chemistry B*, vol. 108, no. 7, pp. 2227–2235, 2004.
- [6] S. Nakade, Y. Saito, W. Kubo, T. Kitamura, Y. Wada, and S. Yanagida, "Influence of TiO<sub>2</sub> nanoparticle size on electron diffusion and recombination in dye-sensitized TiO<sub>2</sub> solar cells," *Journal of Physical Chemistry B*, vol. 107, no. 33, pp. 8607–8611, 2003.
- [7] K. P. Wang and H. S. Teng, "Structure-intact TiO<sub>2</sub> nanoparticles for efficient electron transport in dye-sensitized solar cells," *Applied Physics Letters*, vol. 91, no. 17, Article ID 173102, 3 pages, 2007.
- [8] X. Fang, Y. Bando, U. K. Gautam, C. Ye, and D. Golberg, "Inorganic semiconductor nanostructures and their field-emission applications," *Journal of Materials Chemistry*, vol. 18, no. 5, pp. 509–522, 2008.
- [9] T. Dittrich, E. A. Lebedev, and J. Weidmann, "Electron drift mobility in porous TiO<sub>2</sub> (anatase)," *Physica Status Solidi (A)*, vol. 165, no. 2, pp. R5–R6, 1998.
- [10] M. Law, L. E. Greene, J. C. Johnson, R. Saykally, and P. Yang, "Nanowire dye-sensitized solar cells," *Nature Materials*, vol. 4, no. 6, pp. 455–459, 2005.
- [11] K. Sayama, H. Sugihara, and H. Arakawa, "Photoelectrochemical properties of a porous Nb<sub>2</sub>O<sub>5</sub> electrode sensitized by a ruthenium dye," *Chemistry of Materials*, vol. 10, no. 12, pp. 3825–3832, 1998.
- [12] A. Wold, "Photocatalytic properties of titanium dioxide (TiO<sub>2</sub>)," *Chemistry of Materials*, vol. 5, no. 3, pp. 280–283, 1993.
- [13] R. Hengerer, L. Kavan, P. Krtil, and M. Grätzel, "Orientation dependence of charge-transfer processes on TiO<sub>2</sub> (anatase) single crystals," *Journal of The Electrochemical Society*, vol. 147, no. 4, pp. 1467–1472, 2000.
- [14] H. Deng, H. Zhang, and Z. Lu, "Dye-sensitized anatase titanium dioxide nanocrystalline with (0 0 1) preferred orientation induced by Langmuir-Blodgett monolayer," *Chemical Physics Letters*, vol. 363, no. 5–6, pp. 509–514, 2002.
- [15] P. de Rango, M. Lees, P. Lejay et al., "Texturing of magnetic materials at high temperature by solidification in a magnetic field," *Nature*, vol. 349, no. 6312, pp. 770–772, 1991.
- [16] T. Uchikoshi, "Control of crystalline texture in polycrystalline TiO<sub>2</sub> (Anatase) by electrophoretic deposition in a strong magnetic field," *Journal of the European Ceramic Society*, vol. 26, no. 4–5, pp. 559–563, 2006.
- [17] P. Luo, H. Niu, G. Zheng, X. Bai, M. Zhang, and W. Wang, "Enhancement of photoelectric conversion by high-voltage electric field assisted crystallization of a novel ternary-encapsulated spherical TiO<sub>2</sub> aggregate for solar cells," *Electrochimica Acta*, vol. 55, no. 8, pp. 2697–2705, 2010.
- [18] P. T. Hsiao, Y. L. Tung, and H. Teng, "Electron transport patterns in TiO<sub>2</sub> nanocrystalline films of dye-sensitized solar cells," *Journal of Physical Chemistry C*, vol. 114, no. 14, pp. 6762–6769, 2010.
- [19] N. Koide, A. Islam, Y. Chiba, and L. Han, "Improvement of efficiency of dye-sensitized solar cells based on analysis of equivalent circuit," *Journal of Photochemistry and Photobiology A*, vol. 182, no. 3, pp. 296–305, 2006.



**Hindawi**

Submit your manuscripts at  
<http://www.hindawi.com>

